JACC Vol. 25, No. 5
April 1995:1097–104

Serial Changes in Left and Right Ventricular Systolic and Diastolic Dynamics During the First Year After an Index Left Ventricular Q Wave Myocardial Infarction

KEN HIROSE, MD, PhD, JUDD E. REED, BS, JOHN A. RUMBERGER, PhD, MD, FACC

Rochester, Minnesota

Objectives. **This study quantified serially biventricular emptying and filling after infarction and related these to changes in volume, muscle mass, wall stress and contractility.**

Background. **There are limited data on serial changes in ventricular dynamics after infarction.**

Methods. **Forty patients had serial electron beam computed tomographic examinations during the first year after index Q wave infarction (21 anterior, 19 inferior), and global biventricular volumes, peak rates of emptying and filling and left ventricular muscle masses were quantified. Mean mid–left ventricular end-systolic wall stresses, rate-corrected velocities of circumferential shortening and two indexes of left ventricular contractility—the end-systolic wall stress/volume ratio and the end-systolic wall stress/rate-corrected velocity of circumferential shortening relation—were estimated in each instance.**

Results. **Patients with anterior infarction had an increase in biventricular chamber volume of 15% to 35% by 1 year. Global biventricular peak rates of emptying and filling were decreased by 20% to 30% from hospital discharge to 6 weeks but thereafter remained unchanged. Despite a significant increase in mean wall stresses, the end-systolic wall stress/volume ratio remained unchanged during the year. The rate-corrected velocities of circumferential shortening declined serially after anterior infarction but did so in proportion to the increase in mean wall stresses, consistent with no net change in left ventricular contractility. Patients with inferior infarction showed a trend toward similar changes, but the magnitudes did not reach significance.**

Conclusions. **Left (and right) ventricular global peak rates of emptying and filling during the first year after infarction can be altered in the absence of additional ischemic injury but are more consistent with responses to changes in left ventricular afterload than changes in intrinsic ventricular performance or contractility. Serial changes in left ventricular afterload after infarction are largely due to progressive chamber enlargement and limited development of compensatory hypertrophy during the first year. Intrinsic global left ventricular contractile performance was not altered by postinfarction cardiac remodeling in the patients examined.**

(J Am Coll Cardiol 1995;25:1097–104)

Left (1–5) or right ventricular (6) remodeling, or both, after myocardial infarction has been previously reported, and left ventricular peak rates of systolic emptying and early diastolic filling are known to be depressed chronically after infarction (7–12). However, little is known about the time course of changes in global biventricular systolic emptying and diastolic filling dynamics after infarction and how these may relate to changes in ventricular afterload or contractility, or both. Long-term changes after infarction may include progressive cardiac chamber enlargement, changes in left ventricular shape and wall geometry and development of left ventricular hypertrophy in the noninfarcted myocardium. Such postinfarction ventricular remodeling could contribute to worsening of systolic and diastolic function in the absence of additional ischemic injury, unless compensatory mechanisms remained intact.

To quantify these relations, electron-beam computed tomographic scans from 40 patients at hospital discharge and at 6 weeks, 6 months and 1 year after an index Q wave infarction (21 anterior, 19 inferior) were evaluated to define biventricular chamber volumes, global peak rates of systolic emptying and early diastolic filling, left ventricular muscle masses, and mean mid–left ventricular end-systolic wall stresses and rate-corrected velocities of circumferential fiber shortening. Additionally, two indexes—the end-systolic wall stress/end-systolic volume ratio and the force–velocity relation between left ventricular end-systolic wall stress and rate-corrected velocity of circumferential fiber shortening—were determined to estimate serial changes in global left ventricular contractility associated with postinfarction remodeling.

Methods

Patient selection and entry criteria. Patients admitted to the coronary care unit at the Mayo Clinic within 1 to 3 days of an acute Q wave myocardial infarction, on the basis of clinical, electrocardiographic (ECG) and enzymatic criteria, were identi-

From the Departments of Cardiovascular Diseases and Internal Medicine and Information Services, Mayo Clinic and Foundation, Rochester, Minnesota. This study was supported by an Established Investigator Award to Dr. Rumberger from the American Heart Association, Dallas, Texas and by the Mayo Clinic and Foundation.

Manuscript received February 11, 1994; revised manuscript received September 19, 1994, accepted November 15, 1994.

Address for correspondence: Dr. John A. Rumberger, Department of Cardiovascular Diseases, Mayo Clinic, 200 First Street SW, Rochester, Minnesota 55905.

0735-1097/95/$9.50
0735-1097(94)00014-U

fied as possible candidates for study (5). Patients were ineligible if they had a previous myocardial infarction, historical or physical examination findings consistent with left-sided valvular stenosis or regurgitation graded as moderate or worse, hemodynamic instability, congestive heart failure or renal insufficiency. Concomitant therapy with nitrates, beta-adrenergic blocking agents or calcium channel antagonists was not considered an exclusion criteria. Before entry into the research protocol, each patient signed an institutional review board–approved consent form for serial electron beam computed tomographic studies.

Cardiac imaging. Each patient underwent electron beam computed tomographic (or Ultrafast-CT, Imatron Inc) scanning, as previously described in detail by our laboratory (5,6,13–16). After positioning of the patient to facilitate polytomographic imaging in the transverse cardiac (or "short") axis and assessment of "circulation (or arm–tongue) time" (16), a powered injector delivered an intravenous infusion of nonionic contrast medium (Iopamidol-370, Bristol-Myers Squibb) for 20 s. Imaging, initiated at the ECG R wave, consisted of 13 consecutive frames through the cardiac cycle at six separate tomographic levels (center-to-center distance between levels of 1.0 cm). After a 2- to 5-min interval, the scanning table was moved 6 cm, and the sequence was repeated. The total iodinated contrast load per patient for each imaging session was ~1.5 ml/kg. Patients underwent follow-up scanning at hospital discharge and at 6 weeks, 6 months and 1 year after index myocardial infarction.

Determination of global biventricular peak emptying and filling dynamics, chamber volume and left ventricular muscle masses. The application of electron beam computed tomography to quantitation of early left ventricular diastolic filling has previously been validated (13) and applied to definition of systolic emptying and diastolic filling dynamics in normal subjects and patients with left ventricular volume overload (17). Marzullo et al. (18) have used similar methods to define right ventricular diastolic filling variables. Left and right ventricular endocardial and left ventricular epicardial surfaces were identified and planimetered from each scan acquired through the cardiac cycle (6,15,17,18). Endocardial surface areas were converted to tomographic volumes by multiplying by the center-to-center distance between images, and the data were then entered into a relational data base (17). In the data base, the individual tomographic volumes at all levels from the left ventricular apex through the base of the right ventricular outflow tract at each time, commencing from end-diastole (0% of the cardiac cycle) through systole and up to at least the early rapid filling phase of diastole, were listed in rows. Global left and right ventricular volumes versus time columns were defined by the sums (modified Simpson rule) of each volume at each cardiac time point examined. At normal rest heart rates, data from 13 consecutive 58-ms scan intervals do not necessarily constitute data from an entire cardiac cycle. In those situations, the data were "padded" from the last time point (image 13) to the end-diastolic volume, assuming a linear phase for diastasis as previously described (17). The data were fit to an 8-harmonic Fourier interpolator, and 128 equally spaced points were generated for each individual left and right ventricular volume versus time curve (17). Definition of the timing and slope of the fastest rate of systolic emptying (maximal negative slope) and early diastolic filling (maximal positive slope during rapid filling phase) were determined by calculating the slope on a point-by-point basis for each of the 128 time points. Volumes (and subsequent timing) at end-diastole (largest volume during the cardiac cycle) and end-systole (nadir of the volume during the cardiac cycle) were determined directly from the interpolated volume/time curve. Global left ventricular muscle mass was determined by summing (modified Simpson rule) the end-diastolic tomographic muscle masses (epicardial minus endocardial surface volume) from apex to base, assuming a uniform density for myocardium (1.05 g/ml) (5,6).

Mean end-systolic wall stresses and velocities of fiber shortening at the mid–left ventricular level. A thick-walled Laplacian model was used to estimate mean left ventricular stresses at the equator. Although there were differences in regional left ventricular geometry between the infarcted and noninfarcted myocardium, our purpose was to examine gross changes in mid–left ventricular geometry that could provide insight into serial features of postinfarction remodeling, global wall stresses and contractility to relate to global emptying and filling dynamics. Short-axis tomographic scans representative of approximately the mid–left ventricle, midway between the apical and basal scans, were identified. Features, such as position of papillary muscles and gross characteristics of right ventricular geometry, were compared to allow identification of anatomic sites with distinct similarities for serial studies from each patient. This level corresponded anatomically to the midpapillary muscle level (19) in nearly all instances. For each serial mid–left ventricular scan, the absolute tomographic end-systolic chamber and muscle areas were noted. End-systolic left ventricular meridional (σ_m) and circumferential (σ_c) wall stresses were estimated using formulas originally devised by Mirsky (20) and modified by Douglas et al. (21) (equations 1 and 2, respectively). The advantage of electron beam computed tomography for this application is that muscle mass can be determined accurately, and there are no assumptions regarding global ventricular shape. In the present study, total long-axis left ventricular length at end-systole was determined as the number of left ventricular outflow tract to apex scan levels included in the global volume calculation multiplied by the tomographic image slice thickness (1.0 cm):

$$\sigma_m = 1.33P\frac{\text{LVESA}}{\text{LVSMA}}; \quad [1]$$

$$\sigma_c = 1.33P\frac{\sqrt{\text{LVESA}}}{\sqrt{\text{LVSMA} + \text{LVESA}} - \sqrt{\text{LVESA}}} \times \left[1 - \frac{(4\text{LVESA}\sqrt{\text{LVESA}})/\pi L^2}{\sqrt{\text{LVSMA} + \text{LVESA} + \sqrt{\text{LVESA}}}}\right], \quad [2]$$

where L = total "long-axis" length at end-systole (cm); P = peak systolic arterial (cuff) pressure determined at the time of

scanning; LVESA = mid–left ventricular tomographic end-systolic chamber area (cm^2); and LVSMA = tomographic left ventricular end-systolic muscle area (cm^2). For arterial pressure in mm Hg, wall stresses are calculated as 10^3 dynes/cm^2.

Global left ventricular contractility was estimated using two previously described methods: the end-systolic wall stress/end-systolic volume ratio (22,23) and the end-systolic wall stress and rate-corrected velocity of circumferential fiber shortening relation (24–27). Both methods are generally independent of preload and incorporate afterload (25). Use of rate-corrected velocity of circumferential fiber shortening as a singular index of contractility has been shown to be of limited value because of continued afterload dependence (24–26), but defining both end-systolic wall stress and rate-corrected velocity of circumferential fiber shortening generates a relation that is highly sensitive to changes in actual contractile state (27). Rate-corrected velocity of circumferential fiber shortening was calculated (23,25,26) as follows:

$$Vcf_c = \frac{\%\Delta D}{LVET}\sqrt{RR}; \qquad [3]$$

$$\%\Delta D = \frac{\sqrt{4LVEDA/\pi} - \sqrt{4LVESA/\pi}}{\sqrt{4LVEDA/\pi}},$$

where %ΔD = percent fractional shortening at the left ventricular equator (i.e., midventricle); LVET = left ventricular ejection time (ms); and RR = interval (ms) between consecutive cardiac cycles. Left ventricular ejection time is traditionally a measure of total electromechanical systole. The measurement of total ejection time for mechanical systole was substituted as the time between the maximum to nadir of the systolic left ventricular time-volume curve on the basis of the Fourier interpolated scanning data. Electromechanical coupling time was not available from this noninvasive study. However, no patient had bundle branch block or first-degree atrioventricular block at hospital discharge or during the 1-year follow-up. Rest heart rates ranged within a narrow band in all instances (52 to 82 beats/min). It was therefore presumed that left ventricular ejection time could be calculated and substituted as previously stated because the electromechanical coupling time should have remained relatively invariate in each patient across all serial scans.

Statistical analysis. Data are presented as mean value ± SD. Statistical between-visit comparisons were determined using a repeated-measures analysis of variance with a Student-Neumann-Keuls *t* test for between-visit comparisons. The unpaired Student *t* test was used for comparisons between the subgroups with anterior and inferior wall infarction. A value of $p < 0.05$ for a two-tailed test was considered statistically significant.

Results

Patient demographics. A total of 52 patients were entered into the protocol, but only 48 actually underwent scanning. Of this group, eight patients were excluded from the final analysis (five for incomplete serial scanning, and three for incomplete or suboptimal imaging data). Results are therefore presented for a total of 40 patients (5 women, 35 men; mean [±SD] age 61 ± 10 years, range 44 to 77) who completed four successful electron-beam computed tomographic scans during the first year after index Q wave myocardial infarction (21 anterior, 19 inferior). Interventions at the time of presentation for acute myocardial infarction included urgent percutaneous transluminal coronary angioplasty (11 anterior, 11 inferior), intravenous thrombolytic therapy (9 anterior, 7 inferior) and conventional therapy without initial attempts to establish reperfusion (1 anterior, 1 inferior). As directed by their respective cardiologists, all patients had selective coronary angiography emergently or electively within 1 week of acute infarction, and all had a patent infarct-related coronary artery documented at the termination of the angiographic procedure as a result of thrombolytic therapy or after direct coronary angioplasty, or both. No patient had clinical symptoms of heart failure at presentation to the hospital, at discharge or during follow-up.

Initial scanning was performed within 8 ± 3 days, with serial scans at 58 ± 12, 210 ± 29 and 379 ± 29 days after infarction. For purposes of discussion and in accord with the study protocol, these scan dates are referred to as hospital discharge, 6 weeks, 6 months and 1 year after infarction, respectively. A majority of patients in both infarction subgroups were taking beta-blockers and long-acting nitrates at each visit (16 and 14, respectively, for anterior and 11 and 11, respectively for inferior infarction, p = NS between infarction subgroups). Calcium channel blockers were also taken by ~50% of the patients in each group (10 anterior, 8 inferior infarcts, p = NS). Captopril was taken during the study period in a minority of patients (two anterior vs. two inferior infarcts, p = NS). One patient with an anterior infarction had recurrent angina and underwent a successful second angioplasty of the infarct-related artery at 6 months after infarction; there was no recurrence of angina at 1 year. No patient underwent coronary artery bypass grafting or had a recurrent infarction during follow-up, and all patients were ambulatory.

Hemodynamic variables. Patients were in normal sinus rhythm at all times. Mean heart rate, mean arterial pressure (estimated by cuff), mean global biventricular chamber end-diastolic and end-systolic volumes and global left ventricular muscle mass for each subgroup during the first year are presented in Table 1. Data regarding global left and right ventricular volumes and global left ventricular muscle mass in a smaller sample of these patients have previously been published (5,6). Heart rate was significantly lower and arterial pressure significantly higher at 1 year than at baseline hospital discharge in both subgroups, but comparisons at each scan date between patients with anterior and inferior infarction showed no differences between heart rate and mean arterial pressure. Patients with an anterior infarction demonstrated a progressive increase in left and right ventricular chamber volumes from hospital discharge to 1 year (end-diastolic volume +29% and +15%, respectively; end-systolic volume

Table 1. Comparison of Patients With an Anterior or Inferior Infarction

	Hospital Discharge	6 wk	6 mo	1 yr
Anterior Wall LV Infarction (n = 21)				
HR (beats/min)	70 ± 9	65 ± 10*	63 ± 11*	62 ± 11*
BP (mm Hg)	81 ± 7	84 ± 12	88 ± 13*	93 ± 15*†
LVEDV (ml)	134 ± 25	154 ± 32*	157 ± 26*†	174 ± 31*†‡
LVESV (ml)	65 ± 21	73 ± 21*	75 ± 24*	88 ± 29*†‡
RVEDV (ml)	142 ± 34	152 ± 37*	160 ± 27*	163 ± 30*
RVESV (ml)	73 ± 24	77 ± 19	78 ± 19	89 ± 25*†‡
LV mass (g)	132 ± 27	111 ± 21*	124 ± 32†	134 ± 33†
Inferior Wall LV Infarction (n = 19)				
HR (beats/min)	72 ± 9	64 ± 8*	63 ± 9*	63 ± 9*
BP (mm Hg)	81 ± 7	87 ± 12	81 ± 9	89 ± 15*
LVEDV (ml)	134 ± 20	138 ± 24	145 ± 18	142 ± 25
LVESV (ml)	65 ± 15	62 ± 15	66 ± 17	62 ± 21
RVEDV (ml)	155 ± 32	152 ± 26	151 ± 28	157 ± 28
RVESV (ml)	92 ± 27	84 ± 16	80 ± 17	83 ± 17
LV mass (g)	118 ± 28	110 ± 27§	109 ± 27§	121 ± 22

*$p < 0.05$ versus hospital discharge. †$p < 0.05$ versus 6 weeks. ‡$p < 0.05$ versus 6 months. §$p < 0.05$ versus 1 year. p = NS for all other values. Data presented are mean value ± SD. BP = arterial (cuff) pressure; EDV (ESV) = end-diastolic (end-systolic) volume; HR = heart rate; LV (RV) = left (right) ventricular; mass = myocardial muscle mass.

+35% and +22%, respectively). However, global left ventricular muscle mass reduced significantly during the first 6 weeks after infarction; thereafter, global muscle mass demonstrated a significant trend toward overall increase, returning by 1 year to the value determined at hospital discharge. The decrease in left ventricular muscle mass during the first 6 weeks after infarction was probably due to myocyte loss and dissolution in the infarct region, as discussed elsewhere (5). Global left and right ventricular end-diastolic and end-systolic volumes remained relatively static during the first year in patients with an inferior infarction. Global muscle mass was decreased at 6 weeks but then increased in a pattern similar, although of smaller magnitude, to that observed in the patients with an anterior infarction.

Peak emptying and filling dynamics. Absolute peak emptying and filling rates are functions of ventricular size and overall stroke volume (17). To make comparisons between and among subjects to define systolic and diastolic dynamics, absolute global peak rates of emptying and filling were referenced to the respective absolute global chamber end-diastolic volume (8–11,17,28,29). Table 2 shows serial values for global left and right peak emptying and filling rates (normalized to absolute end-diastolic volume) during the first year after infarction. Previously published normal electron beam com-

Table 2. Serial Values for Global Left and Right Peak Emptying and Filling Rates in Patients With an Anterior or Inferior Infarction

	Normal Values	Hospital Discharge	6 wk	6 mo	1 yr
Anterior Wall LV Infarction (n = 21)					
LV PER/EDV	4.27 ± 0.90	3.61 ± 0.93*	2.57 ± 0.49*†	2.87 ± 0.67*†	2.66 ± 0.77*†
LV PFR/EDV	3.44 ± 1.00	3.34 ± 1.32	2.62 ± 1.08*†	2.37 ± 0.62*†	2.46 ± 0.99*†
RV PER/EDV		3.29 ± 1.43	2.56 ± 0.36†	2.54 ± 0.48†	2.45 ± 0.55†
RV PFR/EDV	2.7 ± 0.4	2.67 ± 1.88	2.09 ± 0.56*	1.96 ± 0.51*	2.01 ± 0.79*
Inferior Wall LV Infarction (n = 19)					
LV PER/EDV	4.27 ± 0.90	3.39 ± 0.94*	3.33 ± 0.79*	3.09 ± 0.69*	3.06 ± 0.56*
LV PFR/EDV	3.44 ± 1.00	3.16 ± 1.42	2.63 ± 1.00*	2.43 ± 0.47*	2.44 ± 0.63*
RV PER/EDV		2.49 ± 0.74	2.40 ± 0.51	2.41 ± 0.46	2.41 ± 0.42
RV PFR/EDV	2.7 ± 0.4	2.21 ± 1.15	1.77 ± 0.36*	1.89 ± 0.50*	1.87 ± 0.40*

*$p < 0.05$ versus normal values. †$p < 0.05$ versus hospital discharge. Normal values are from Rumberger and Reed (17) (n = 15) and Marzullo et al. (18) (n = 10). Data presented are mean value ± SD. PER (PFR)/EDV = peak emptying (filling) rate normalized to absolute end-diastolic volume (1/s); other abbreviations as in Table 1.

Table 3. Comparison of Global Left Ventricular Systolic Function and Wall Stresses in Patients With an Anterior or Inferior Infarction

	Hospital Discharge	6 wk	6 mo	1 yr
Anterior Wall LV Infarction (n = 21)				
LV SV (ml)	70 ± 16	78 ± 22	82 ± 15*	87 ± 17*
RV SV (ml)	67 ± 16	74 ± 23	81 ± 20	76 ± 16
LV EF (%)	0.52 ± 0.11	0.52 ± 0.12	0.53 ± 0.11	0.51 ± 0.12
RV EF (%)	0.48 ± 0.11	0.48 ± 0.09	0.51 ± 0.08	0.46 ± 0.09
LV σ_m	77 ± 29	98 ± 41*	96 ± 42*	106 ± 47*
LV σ_c	203 ± 62	254 ± 90*	254 ± 91*	271 ± 101*
LV σ_m/ESV	1.29 ± 0.45	1.45 ± 0.49	1.31 ± 0.36	1.28 ± 0.32
LV σ_c/ESV	3.51 ± 1.16	3.86 ± 1.31	3.64 ± 0.92	3.35 ± 0.79
LV Vcf_c	0.83 ± 0.38	0.70 ± 0.29*	0.69 ± 0.26*	0.68 ± 0.24*
Inferior Wall LV Infarction (n = 19)				
LV SV	69 ± 20	75 ± 18	78 ± 12	80 ± 18
RV SV	64 ± 22	68 ± 16	71 ± 21	74 ± 19
LV EF	0.52 ± 0.10	0.55 ± 0.08	0.54 ± 0.08	0.56 ± 0.10
RV EF	0.42 ± 0.12	0.45 ± 0.07	0.48 ± 0.08	0.47 ± 0.08
LV σ_m	82 ± 39	89 ± 36	90 ± 36	84 ± 37
LV σ_c	208 ± 78	238 ± 78	239 ± 80	225 ± 81
LV σ_m/ESV	1.33 ± 0.45	1.44 ± 0.38	1.43 ± 0.47	1.35 ± 0.26
LV σ_c/ESV	3.40 ± 0.86	3.90 ± 0.89	3.79 ± 0.96	3.73 ± 0.63
LV Vcf_c	0.74 ± 0.22	0.74 ± 0.23	0.74 ± 0.19	0.77 ± 0.21

*$p < 0.05$ versus hospital discharge. p = NS for all other values. Data presented are mean value ± SD. EF = ejection fraction (%); SV = global stroke volume (ml); Vcf_c = rate-corrected velocity of circumferential fiber shortening (circumferences/s); σ_c (σ_m) = end-systolic equatorial, mean circumferential (meridional) wall stress (10^3 dynes/cm^2); σ_c/ESV (σ_m/ESV) = end-systolic circumferential (meridional) wall stress/global left ventricular end-systolic volume (10^3 dynes/cm^2 per ml); other abbreviations as in Table 1.

puted tomographic values for the left (17) and right (18) ventricles are shown for reference. At hospital discharge after anterior infarction, left ventricular peak emptying rate was slightly lower than normal, but left and right ventricular peak filling rates were normal. By 6 weeks, biventricular systolic emptying and diastolic filling rates were reduced by 20% to 30% and were significantly below normal. Furthermore, left ventricular emptying and filling and right ventricular emptying rates were significantly depressed compared with those at hospital discharge. Thereafter, throughout the 1-year follow-up, these values remained essentially unchanged. In contrast, left ventricular emptying and filling and right ventricular filling rates after inferior infarction were not statistically different during the first year after infarction compared with those at hospital discharge despite a trend for differences similar to those seen after anterior infarction between discharge and 1 year. Right ventricular emptying rate after inferior infarction showed no change during the first year. Left ventricular emptying rate was significantly lower at 6 weeks after anterior than inferior infarction ($p < 0.001$). By contrast, right ventricular emptying rate at hospital discharge and filling rate at 6 weeks were significantly lower after inferior than anterior infarction ($p = 0.015$ and $p = 0.042$, respectively).

Global left ventricular systolic function and wall stress. Global biventricular stroke volumes, ejection fraction, mean mid–left ventricular end-systolic meridional and circumferential wall stresses, wall stress/end-systolic volume ratios and rate-corrected velocities of circumferential fiber shortening for both anterior and inferior infarction are shown in Table 3. Global left and right ventricular stroke volumes remained unchanged during the first year in both groups, except that global left ventricular stroke volume increased significantly at 6 months and 1 year compared with that at hospital discharge in patients with an anterior wall infarction. Global left and right ventricular ejection fractions remained unchanged after hospital discharge in both groups. Although mid–left ventricular end-systolic meridional and circumferential wall stresses in patients with an anterior wall infarction increased progressively and significantly during the first year, there were no significant changes in serial end-systolic meridional and circumferential wall stress/end-systolic volume ratios in either group during the first year. However, rate-corrected velocity of circumferential fiber shortening was significantly depressed at 6 weeks compared with that at hospital discharge in patients with an anterior wall infarction. No significant changes were noted in patients with an inferior wall infarction during the 1-year study period. When patients with an anterior versus inferior wall infarction are compared, global biventricular stroke volumes, ejection fractions, end-systolic wall stresses and rate-corrected velocities of circumferential fiber shortening were not significantly different at any time during the study period.

JACC Vol. 25, No. 5
April 1995:1097–104

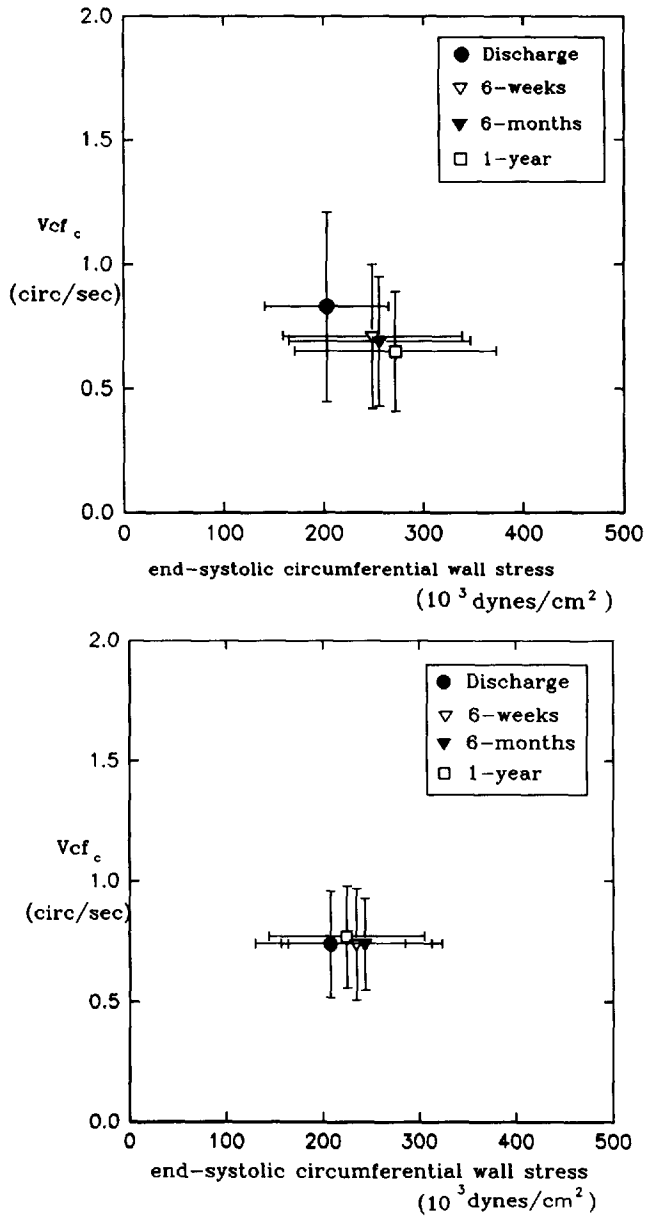

Figure 1. Mean end-systolic circumferential wall stress/rate-corrected velocity of fiber shortening (Vcf_c) data during the first year after an anterior (**top** [n = 21]) and inferior (**bottom** [n = 19]) wall myocardial infarction. Data are mean value ± SD. circ/sec = circumferences per second; Discharge = hospital discharge.

Relation between left ventricular wall stress and velocity of circumferential fiber shortening. Because rate-corrected velocity of circumferential fiber shortening approximates the summed effect of shortening in the circumferential direction, the more quantitatively correct measure of left ventricular afterload would be to correlate it with the wall stress acting in the same ventricular plane. The end-systolic (circumferential) wall stress/rate-corrected velocity of circumferential fiber shortening relation during the year is shown in Figure 1 for anterior (top) and inferior (bottom) infarction. Serial estimates of the end-systolic wall stress/rate-corrected velocity of circumferential fiber shortening relation in patients with an anterior infarction show a rightward and downward shift in the data points during the 1-year follow-up. Therefore, when afterload was eliminated as a confounding variable, serial decreases in the rate-corrected velocity of circumferential fiber shortening after anterior infarction were consistent with a physiologically appropriate response to concomitant serial increases in left ventricular end-systolic wall stress (afterload). For patients with an inferior infarction, the end-systolic wall stress/rate-corrected velocity of circumferential fiber shortening relation remained unchanged during the year after infarction.

Discussion

There are three major conclusions from the current investigation. First, in patients with an anterior infarction, there was a significant decline in peak global left and right ventricular emptying and filling rates at hospital discharge to the 6-week follow-up. Thereafter, peak emptying and filling rates remained essentially unchanged. There was a trend for similar changes in patients with an inferior infarction that did not reach statistical significance. At first glance this could suggest that the decline in emptying and filling dynamics after hospital discharge in patients with an anterior infarction could be consistent with a parallel decline in ventricular performance; however, as shown in Table 3, ejection fraction or stroke volume, or both, remained unchanged or even increased during the year after infarction in both groups.

Second, despite disparate changes in biventricular volumes, global emptying and filling dynamics and equatorial end-systolic wall stresses, two separate indexes suggested that intrinsic left ventricular contractility was unchanged during the first year in both groups. In particular, rate-corrected velocities of circumferential fiber shortening decreased serially after anterior wall infarction but did so as equatorial wall stresses increased. The end-systolic wall stress/rate-corrected velocity of circumferential fiber shortening relation altered in a manner consistent with afterload dependence, not a change in global left ventricular contractility. Additionally, the end-systolic wall stress/end-systolic volume ratio, another index of contractility, remained unchanged from hospital discharge throughout the first year after infarction. Thus, further depression in normal peak emptying and filling rates after infarction, in the absence of additional ischemic injury, are consistent with changes in left (and possibly right) ventricular loading conditions and not necessarily changes in intrinsic left (and right) ventricular performance or contractility.

Third, increases in left (and probably right) ventricular afterload are in great part caused by dynamic changes in ventricular chamber volumes accompanied by limited development of compensatory left ventricular hypertrophy during the first year after infarction. These data support the contention that intrinsic left ventricular contractile and filling performance during the first year after an uncomplicated myocardial infarction is not altered by postinfarction cardiac remodeling.

Finally, the data are internally consistent in the finding that the patients with an inferior versus anterior infarction had little subsequent remodeling after discharge and, thus, little subsequent changes in wall stresses (despite elevations in mean aortic pressure by 1 year), emptying and filling dynamics and rate-corrected velocities of circumferential shortening.

Study limitations. There are several limitations of the current study that bear on its interpretation. First, the number of patients was small, and differences were seen mainly in those with anterior infarction. The sample sizes were similar, but because of probably smaller areas of ventricular necrosis, more patients may have been needed to define statistically significant differences in patients with inferior infarction. Data from our laboratory have confirmed that infarct size at hospital discharge is a major determinant of the magnitude of ventricular remodeling at 1 year after infarction (30). Second, the patients studied represent only a subpopulation of patients surviving an index infarction in that none had heart failure (by study design), and all had patent infarct-related coronary arteries at hospital discharge. If infarct-related artery patency has an independent effect on the extent of ventricular chamber dilation after infarction (31–33), then the magnitude of changes seen in this study are an underestimation of the extent of remodeling that could occur in some patients. Whether the "open artery" observations represent an epiphenomenon or an important pathophysiologic mechanism remains to be completely addressed. Because we did not have a companion group with nonpatent infarct-related arteries at hospital discharge, this issue cannot be addressed by the current study design.

Determinations of biventricular volumes and left ventricular muscle masses by electron-beam computed tomography are among the most accurate possible in any experimental population (13,16,17). Thus, no significant errors in serial definition of chamber volume and muscle mass are considered that could influence the results as presented. Patient hemodynamic variables in Table 1 remained at all times within the expected norms for a random adult patient group, but heart rates and mean arterial pressures were different at the end of the study from those at the beginning. The magnitude of the effect of these slight differences in loading conditions on ventricular dynamics would be difficult to predict but could explain some of the observed increases in ventricle chamber volumes and wall stresses noted during the 1-year follow-up period. However, these minimal differences would not be expected to explain fully the patterns displayed in Tables 2 and 3. Patients with inferior infarction also had an increase in mean arterial pressure at 1 year (Table 1) but no increase in wall stresses. Beta-blockers (34), calcium channel antagonists (35) and long-acting nitrates (36) may have a variable effect on peak emptying and filling dynamics and have been implicated in either limiting the development of left ventricular hypertrophy (37) or the extent of ventricular dilation (38). Four patients received an angiotensin-converting enzyme inhibitor after infarction, and this may have limited the extent to which the ventricles dilated after infarction (39). Because the majority of patients were taking the same medications prescribed at discharge throughout the study period, it is assumed that if any pharmacologic effects were contributory to the results, the magnitude of this contribution was consistent on serial follow-up. We evaluated only the first year after infarction, when no patient had clinical heart failure. However, if wall stresses continue to increase remote from the date of infarction, then there may eventually be further alterations in left ventricular performance representative of changes in intrinsic contractility, as suggested in patients with dilated cardiomyopathy (37). Gaudron et al. (3) have shown that patients with uncomplicated large infarctions were beginning to show a decline in left ventricular ejection fraction at 3 years after infarction.

Quantification of ventricular wall stresses can be problematic because there currently exist no completely satisfactory formulations, except for finite element methods, which require precise and simultaneous quantification of intracavity pressures (40,41). Most previous clinical studies have been based on definition of ventricular geometry, generally at the equator, requiring dimensions, such as cavity length, local radius of chamber curvature and wall thicknesses (20,42,43). Several formulations have been put forward for calculation of regional wall stresses that account for differences in regional wall thicknesses, the most notable being that of Janz et al. (44), but this method, like others, has its limitations. However, despite the fact that the magnitudes for wall stresses reported here are in agreement with values reported by others, both in patients with myocardial infarction and those with dilated cardiomyopathy, absolute quantification of regional wall stresses around the midventricular circumference was not the primary goal of this investigation. The use of a thick-walled Laplacian model is admittedly an oversimplification of the situation. In the current study we examined global left ventricular performance characteristics and used a spatially averaged approach to define equatorial wall stresses and indexes of contractility, and these limitations may affect our interpretations of the data. Although the use of such methods does not provide insight into regional dynamics associated with postinfarction cardiac remodeling, it should be considered a valid first approximation to the changes that occur in the left ventricle as a whole.

References

1. Pfeffer MA, Braunwald E. Ventricular remodeling after myocardial infarction. Circulation 1990;81:1161–72.
2. Erlebacher JA, Weiss JL, Eaton LW, Kallman C, Weisfeldt ML, Bulkley BH. Late effects of acute infarct dilation on heart size: a two-dimensional echocardiographic study. Am J Cardiol 1982;49:1120–6.
3. Gaudron P, Eilles C, Kugler I, Ertl G. Progressive left ventricular dysfunction and remodeling after myocardial infarction. potential mechanisms and early predictors Circulation 1993;87:755–63.
4. Mitchell GF, Lamas GA, Vaughan DE, Pfeffer MA. Left ventricular remodeling in the year after first anterior myocardial infarction: a quantitative analysis of contractile segment lengths and ventricular shape. J Am Coll Cardiol 1992;19:1136–44.
5. Rumberger JA, Behrenbeck T, Breen JR, Reed JE, Gersh BJ. Nonparallel changes in global left ventricular chamber volume and muscle mass during the first year after transmural myocardial infarction in humans. J Am Coll Cardiol 1993;21:673–82.
6. Hirose K, Shu NH, Reed JE, Rumberger JA. Right ventricular dilatation and

remodeling the first year after an initial transmural wall left ventricular myocardial infarction. Am J Cardiol 1993;72:1126–30.
7. Finkelhor RS, Sun JP, Bahler RC. Left ventricular filling shortly after an uncomplicated myocardial infarction as a predictor of subsequent exercise capacity. Am Heart J 1990;119:85–91.
8. Bonow RO, Bacharach SL, Green MV, et al. Impaired left ventricular diastolic filling in patients with coronary artery disease: assessment with radionuclide angiography. Circulation 1981;64:315–23.
9. Fujii J, Yazaki Y, Sawada H, Aizawa T, Watanabe H, Kato K. Noninvasive assessment of left and right ventricular filling in myocardial infarction with a two-dimensional Doppler echocardiographic method. J Am Coll Cardiol 1985;5:1155–60.
10. Isobe M, Yazaki Y, Takaku F, et al. Right ventricular filling detected by pulsed Doppler echocardiography during the convalescent stage of inferior wall acute myocardial infarction. Am J Cardiol 1987;59:1245–50.
11. Johannessen KA, Cerqueria MD, Stratton JR. Influence of myocardial infarction size on radionuclide and Doppler echocardiographic measurements of diastolic function. Am J Cardiol 1990;65:692–7.
12. Aoyagi T, Pouleur H, Eyll VC, Rousseau MF, Mirsky I. Wall motion asynchrony is a major determinant of impaired left ventricular filling in patients with healed myocardial infarction. Am J Cardiol 1993;72:268–72.
13. Rumberger JA, Weiss R, Feiring AJ, et al. Patterns of regional diastolic function in the normal human left ventricle: an ultrafast computed tomographic study. J Am Coll Cardiol 1989;14:119–26.
14. Rumberger JA, Bell MR, Stanson AF, Sheedy PF, Behrenbeck T. Assessment of left ventricular diastolic function in man using ultrafast computed tomography. Am J Cardiac Imag 1990;4:130–7.
15. Reiter SJ, Rumberger JA, Feiring AJ, Stanford W, Marcus ML. Precision of right and left ventricular stroke volume measurements by rapid acquisition cine computed tomography. Circulation 1986;74:890–900.
16. Rumberger JA, Behrenbeck T, Sheedy PF, Stanton AW. Ultrafast computed tomography. In: Giuliani ER, Fuster V, Gersh BJ, McGoon DC, editors. Cardiology Fundamentals and Practices. St. Louis: Mosby-Year Book, 1991:387–97.
17. Rumberger JA, Reed JE. Quantitative dynamics of left ventricular emptying and filling as a function of heart size and stroke volume in pure aortic regurgitation and in normal subjects. Am J Cardiol 1992;70:1045–50.
18. Marzullo P, L'Abbate A, Marcus M. Patterns of global and regional systolic and diastolic function in the normal right ventricular assessed by ultrafast computed tomography. J Am Coll Cardiol 1991;17:1318–25.
19. Feiring AJ, Rumberger JA, Reiter SJ, et al. Sectional and segmental variability of left ventricular function: experimental and clinical studies using ultrafast computed tomography. J Am Coll Cardiol 1988;12:415–25.
20. Mirsky I. Review of various theories for evaluation of left ventricular wall stress. In: Mirsky I, Chiston DN, Sandler H, editors. Cardiac Mechanics: Physiological, Chemical and Mathematical Considerations. New York: Wiley, 1974:381–409.
21. Douglas PS, Morrow R, Alfred I, Reichek N. Left ventricular shape, afterload and survival in idiopathic dilated cardiomyopathy. J Am Coll Cardiol 1989;13:311–5.
22. Carabello BA. Ratio of end-systolic stress to end-systolic volume: is it a useful clinical tool? J Am Coll Cardiol 1989;14:496–8.
23. Kimball TR, Daniels SR, Loggie JMH, Khoury PK, Meyer RA. Relation of left ventricular mass, preload, afterload and contractility in pediatric patients with essential hypertension. J Am Coll Cardiol 1993;21:997–1001.
24. Colan SD, Borow KM, Neuman NA. Left ventricular end-systolic wall stress–velocity of fiber shortening relation: a load-independent index of myocardial contractility. J Am Coll Cardiol 1984;4:715–24.
25. Borow KM. Clinical assessment of contractility in the symmetrically contracting left ventricle. Mod Concepts Cardiovasc Dis 1988;57:29–34.
26. Lang RM, Pridjian G, Feldman T, Neumann A, Lindheimer M, Borow KM. Left ventricular mechanics in preeclampsia. Am Heart J 1991;121:1768–75.
27. Borow KM, Neumann A, Marcus RH, Sareli P, Lang RM. Effects of simultaneous alterations in preload and afterload on measurements of left ventricular contractility in patients with dilated cardiomyopathy: comparisons of ejection phase, isovolumetric and end-systolic force-velocity indexes. J Am Coll Cardiol 1992;20:787–95.
28. Bareiss P, Facello A, Constantinesco A, et al. Alterations in left ventricular diastolic function in chronic ischemic heart failure: assessment by radionuclide angiography. Circulation 1990;81 Suppl III:III-71–7.
29. Verani MS, Guidry GW, Mahmarian JJ, et al. Effects of acute, transient coronary occlusion on global and regional right ventricular function in humans. J Am Coll Cardiol 1992;20:1490–7.
30. Chareonthaitawee P, Christian TF, Hirose K, Gibbons RJ, Rumberger JA. The relationship of infarct size with the extent of left ventricular remodeling following myocardial infarction [abstract]. Circulation 1993;88 Suppl I:I-639.
31. Christian TF, Behrenbeck T, Gersh BJ, Gibbons RJ. Relation of left ventricular volume and function over one year after acute myocardial infarction to infarction size determine by technicium-99m sestamibi. Am J Cardiol 1991;68:21–6.
32. Warren SE, Rayal HD, Markis JE. Time course of left ventricular dilation after myocardial infarction: influence of infarct-related artery and success of coronary thrombosis. J Am Coll Cardiol 1988;11:12–7.
33. Braunwald E. Myocardial reperfusion, limitation of infarct size, reduction of left ventricular dysfunction and improved survival: should the paradigm be expanded? Circulation 1989;79:441–2.
34. Fouad FM, Soliminiski MJ, Tarazi RC, Gallagher JH. Alterations in left ventricular filling with beta-adrenergic blockade. Am J Cardiol 1983;51: 161–4.
35. Bonow RO. Effects of calcium-channel blocking agents on left ventricular diastolic function in hypertrophic cardiomyopathy and in coronary artery disease. Am J Cardiol 1985;55:172B–8B.
36. Plotnick GD, Hahn B, Rogers WJ, Fisher ML, Becker LC. Effect of postural changes, nitroglycerin and verapamil on diastolic ventricular function as determined by radionuclide angiography in normal subjects. J Am Coll Cardiol 1988;12:121–9.
37. McDonald KM, Carlyle PF, Francis GS, Cohn JN. The comparative effects of beta-adrenoceptor blockade and angiotensin converting enzyme inhibitor therapy on established ventricular remodeling in the dog [abstract]. Am J Hypertens 1993;6:14A.
38. McDonald KM, Francis GS, Matthews J, Hunter D, Cohn JN. Long-term oral nitrate therapy prevents chronic ventricular remodeling in the dog. J Am Coll Cardiol 1993;21:514–22.
39. Pfeffer MA, Lamas GA, Vaughan DE, Parisi AF, Braunwald E. Effect of captopril on progressive ventricular dilatation after anterior myocardial infarction. N Engl J Med 1988;319:80–6.
40. Janz RF, Brimm AF. Finite-element model for the mechanical behavior of the left ventricle. Circ Res 1972;30:244–52.
41. McPherson DD, Skorton DJ, Kodiyalam S, et al. Finite element analysis of myocardial diastolic function using three-dimensional echocardiographic reconstructions: application of a new method for study of acute ischemia in dogs. Circ Res 1987;60:674–82.
42. Grossman W, Jones D, McLaurin LP. Wall stress and patterns of hypertrophy in the human left ventricle. J Clin Invest 1975;56:56–64.
43. Falsetti HL, Mates RE, Grant C, Greene DG, Bunnell IL. Left ventricular wall stress calculated from one-plane cineangiography. Circ Res 1970;26:71–83.
44. Janz RF, Ozpetek S, Binzton LE, Laks MM. Regional stress in a noncircular cylinder. Biophys J 1989;55:173–82.